acoustics

MDPI

Article

A Frequency-Independent Phase Shifter

Máté Csanád [1], Amira K. F. Val Baker [2,*] and Paul Oomen [2]

[1] Department of Atomic Physics, Eötvös Loránd University, 1117 Budapest, Hungary; csanad@elte.hu
[2] Research & Development Department, The Works Research Institute B. V., 1015 Amsterdam, The Netherlands; poomen@theworks.info
* Correspondence: avbaker@theworks.info

Abstract: In this paper, we utilise optimization methods to determine a frequency-independent phase shift such that two phase-shifted versions of a signal can be summed and the resulting amplitude spectrum is unchanged. A phase difference between two signals is thus defined, which remains constant for all frequencies within a given range. For the intended purpose of this study, we set the frequency range to the audible human hearing range of 16 Hz–20 kHz. We found that a new 3-stage filter method provides a variable phase shifter (i.e., ϕ = 0–360°) without the need for additional amplifiers. In addition, we present a new method that reduces the number of filters necessary, improving both the accuracy and efficiency of current techniques.

Keywords: band filter; signal processing; sound transformation; phase shifter; time delayer; frequency independence

check for updates

Citation: Csanád, M.; Val Baker, A.K.F.; Oomen, P. A Frequency-Independent Phase Shifter. *Acoustics* **2024**, *6*, 713–729. https://doi.org/10.3390/acoustics6030039

Academic Editors: Fengshou Gu and Jian Kang

Received: 26 May 2024
Revised: 17 July 2024
Accepted: 26 July 2024
Published: 31 July 2024

1. Introduction

Phase shifters change the output phase angle of an input signal and are thus utilised in many areas of electronics, instrumentation, and signal processing [1–6].

The most commonly used types of phase shifters are, in fact, time delayers, which introduce a frequency-independent time delay. Depending on the intended application of the phase shifter, it is important to consider how the amplitude response is affected. For example, when controlling variable response angles in a spatially distributed microphone array, microphone signals are combined and phase-shifted [7–10]. It is therefore important that the phase shift is independent of the frequency, such that the amplitude response is equal for all frequencies and the resulting amplitude spectrum of the signal is unchanged. However, such frequency-independent phase shifters are more complex in their technical design and have yet to be optimally developed. For example, a traditional phase shifter in which the phase shift is changed manually can be used to achieve a frequency-independent phase shift [1,11,12]. These methods can then be automated with the use of a programmable variable resistor [13–18]. However, they are only operational either at single frequencies [16] or specific frequency ranges, but at a lower accuracy [17]. They can also require multiple stages [18].

For a frequency-independent phase shift of 90° ($\pi/2$ in radians), a comprehensive analytical solution is given by the Hilbert Transform. The Hilbert Transform can be understood as first transforming into the frequency domain by applying a FFT and then phase-shifting all positive frequency spectral components by $-90°$ and all negative frequency spectral components by +90°. Then, by applying the inverse FFT, a time domain phase-shifted spectrum is obtained where the amplitude spectrum is unchanged. However, this solution is purely analytical, and no straightforward implementation exists analogously in signal processing. Implementation is thus carried out by passing the signal through various stages of filters, i.e., band-pass filters and all-pass filters. Various strategies for implementation can be found that may differ greatly based on the intended application, and each has their own limitations and drawbacks. For example, [18] implements the

Hilbert transform via a two-stage filter and a five-stage filter. In both cases, a flat response was achieved for a specific frequency range of ω = 55 Hz–2 kHz and a phase angle of $\phi = 34°$, as well as for ω = 100 Hz–20 kHz, $\phi = -30°$, respectively. This approach works well, but is costly in terms of implementation and only allows fixed phase shifts for a limited frequency range. Another approach allows for a variable phase shift, i.e., ω = 16 Hz–20 kHz, $\phi = 0$–$360°$, by implementing a Hilbert transform via a 2 × 3-stage filter and three additional amplifiers [10]. In this approach, the added functionality and range come at further added computational costs.

It is evident that the current methods utilised to achieve frequency-independent phase shifts require substantial complexity in the technical design and involve multiple filters, thus limiting efficiency. In this paper, we utilise optimization methods to determine a frequency-independent phase shift. We describe a three-stage filter that provides a variable phase shifter, i.e., $\phi = 0$–$360°$, without the need for additional amplifiers. In addition, we present a new method that reduces the number of filters necessary, improving on both the accuracy and efficiency of current techniques.

2. Materials and Methods

An all-pass filter is a filter that introduces a phase shift while not affecting the amplitude response of a signal. They are typically designed using operational amplifiers and discrete resistors and capacitors. See Figure 1a for an example of a first-order all-pass filter and Figure 1b for an example of a second-order all-pass filter. Note that both examples are for a phase shift variation from $-180°$ (at 0 Hz) to $0°$ (at higher frequencies), where, at $\omega = 1/RC$, the value of the phase shift is $-90°$.

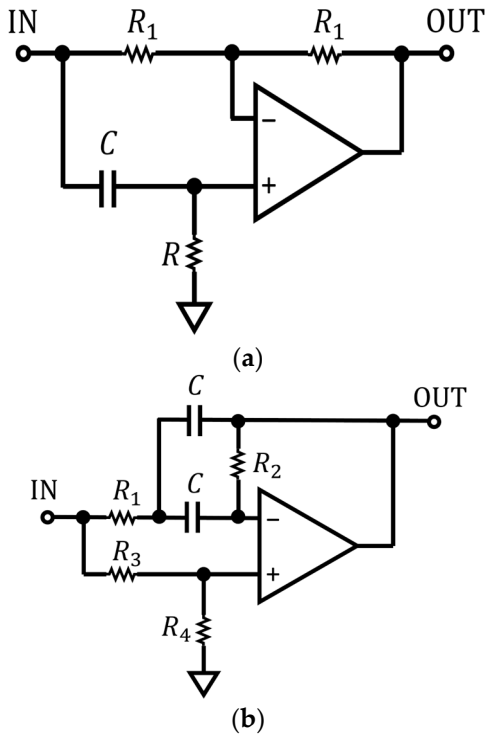

Figure 1. Implementation of (**a**) a first-order and (**b**) a second-order all-pass filter.

These circuits are only operational at a single frequency, where each component is chosen specifically for a phase shift at a given frequency. If we want to adapt such a system to a phase shift for variable frequency, we have to make the circuit frequency-independent using variable components, e.g., programmable resistors and capacitors; voltage control resistors (VCR); and Junction-gate Field Effect Transistors (JFET). For an example, see Figure 2.

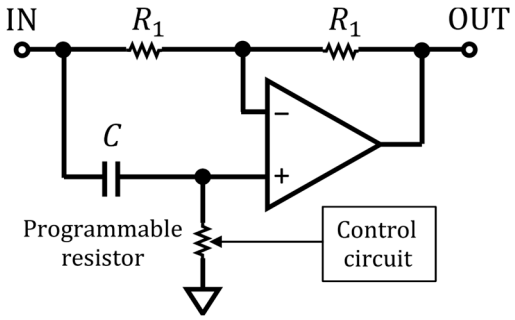

Figure 2. Implementation of a frequency-independent phase shifter.

An all-pass filter can also be implemented digitally; see Figure 3 for an example of a digitally implemented (Figure 3a) first-order and (Figure 3b) second-order all-pass filter.

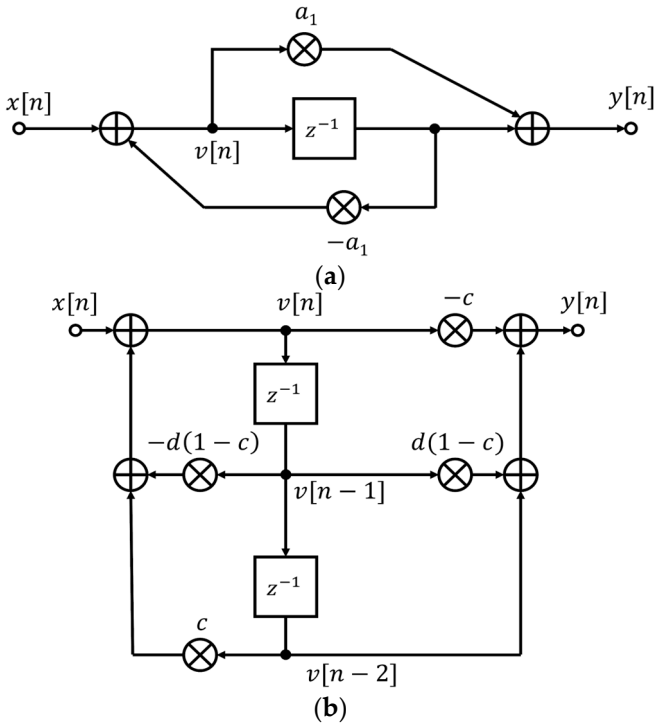

Figure 3. Digital implementation of a (**a**) first-order and (**b**) second-order all-pass filter, where *x[n]* is the input signal; *y[n]* is the output signal; *v[n]* is the difference equation; Z^{-1} is the signal in the complex domain; and a, c, and d are parameters that control the break frequency, bandwidth, and cutoff frequency.

We can then use an all-pass filter to achieve a band-stop filter where the frequency range is determined by a centre frequency, ω_0, and a bandwidth, BW, defined by the Q-factor:

$$Q = \frac{\omega_0}{BW}. \tag{1}$$

The band-stop filter is a combination of a low-pass filter and a high-pass filter with identical cut-off frequencies, corresponding to ω_0 above (see Figure 4).

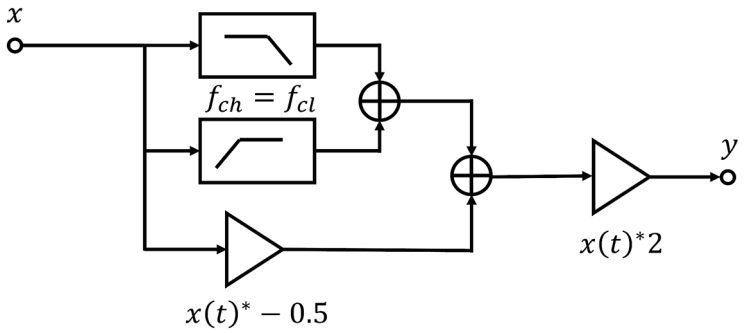

Figure 4. An all-pass band-stop filter, where x is the input signal; y is the output signal; and f_{ch} and f_{cl} are the higher and lower cutoff frequencies, respectively.

A first-order all-pass band-stop filter can be used to achieve a signal with a uniform amplitude response and a phase response ϕ as a function of frequency ω, expressed as

$$\phi(\omega) = -4 \cdot atan(\omega/\omega_0) \tag{2}$$

Note that the addition of the low-pass and high-pass filters results in a maximum phase shift range of 360° (i.e., −4atan).

The second-order filter allows a variable bandwidth with a phase response by introducing the Q-factor as a new parameter:

$$\phi(\omega) = -4 \cdot atan\left[(\omega/\omega_0)^{-Q}\right] \tag{3}$$

See Figure 5 for the resulting phase shifts for ω_0 = 500 Hz and Q = 0.5–2.0.

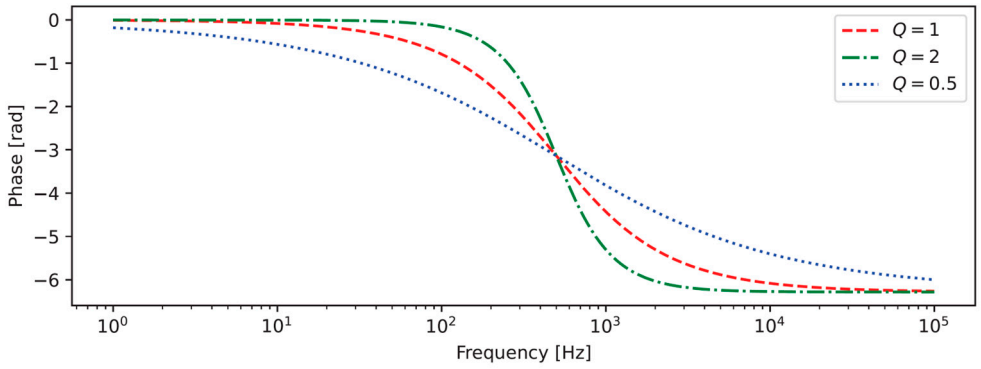

Figure 5. Phase shift as a function of frequency, with ω_0 = 500 Hz and Q = 0.5–2.0.

A combination of several such phase shifters can also be utilised. For example, one can take a phase shifter (A) of three components:

$$\begin{aligned}\phi_A(\omega) = -4 \cdot atan\left[(\omega/\omega_{0,1,A})^{-Q_{1,A}}\right] - 4 \cdot atan\left[(\omega/\omega_{0,2,A})^{-Q_{2,A}}\right] \\ -4 \cdot atan\left[(\omega/\omega_{0,3,A})^{-Q_{3,A}}\right]\end{aligned} \tag{4}$$

with parameters

$$\omega_{0,1,A} = 16\ Hz,\ \ \omega_{0,2,A} = 320\ Hz,\ \omega_{0,3,A} = 6400\ Hz,$$

and

$$Q_{1,A} = Q_{2,A} = Q_{3,A} = 0.707$$

and another phase shifter (B):

$$\phi_B(\omega) = -4{\cdot}atan\left[(\omega/\omega_{0,1,B})^{-Q_{1,B}}\right] - 4{\cdot}atan\left[(\omega/\omega_{0,2,B})^{-Q_{2,B}}\right] - 4{\cdot}atan\left[(\omega/\omega_{0,3,B})^{-Q_{3,B}}\right], \quad (5)$$

with parameters

$$\omega_{0,1,B} = 35\ Hz,\ \omega_{0,2,B} = 700\ Hz,\ \omega_{0,3,B} = 14,000\ Hz,$$

and

$$Q_{1,B} = Q_{2,B} = Q_{3,B} = 0.707,$$

and obtain the total phase shift as

$$\phi(\omega) = \phi_A(\omega) - \phi_B(\omega). \quad (6)$$

The individual $\phi_A(\omega)$ and $\phi_B(\omega)$ phase shifts are shown in Figure 6.

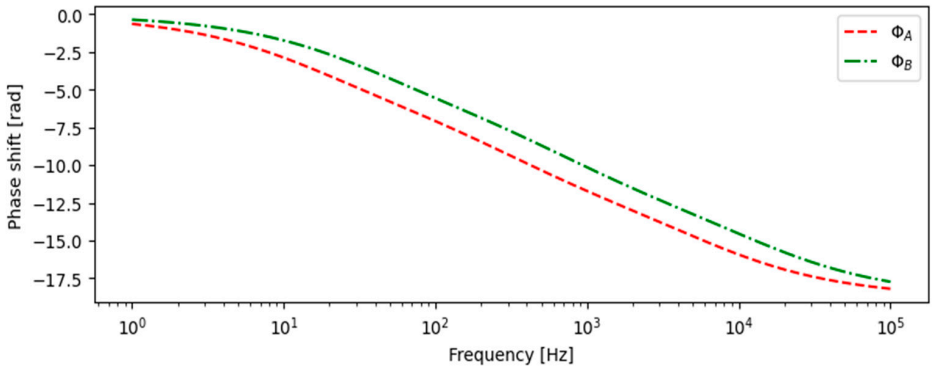

Figure 6. Phase shift as a function of frequency for two three-stage filters with two different sets of parameters.

The difference in these phase shifts, $\phi(\omega)$, is more or less constant in the 30 Hz to 6 kHz range, but exhibits substantial variation even within that range. Outside that range, the phase shift changes even more (see Figure 7).

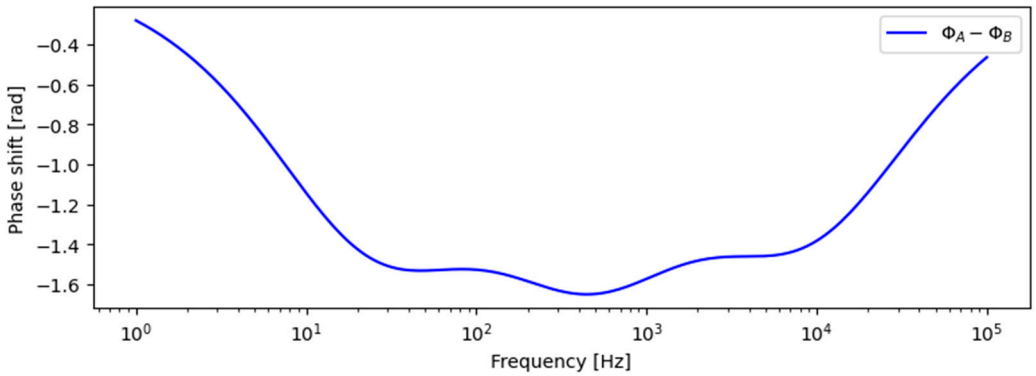

Figure 7. Phase difference as a function of frequency for a filter with two three-stage filters. The function shown in this plot is the difference of the two functions shown in Figure 6.

In the following section, we describe the optimization of such filters with one or more stages, with parameters optimised numerically and analytically as well. The former method usually yields more accurate results, while the latter helps in guiding the analysis and obtaining a more detailed qualitative understanding.

3. Results

3.1. Numerical Optimization of a Single-Stage Filter

To achieve a more constant phase shift as compared to the default version discussed above, we can numerically optimise the parameters by minimising the deviation from a constant $\phi(\omega) = \phi_0$, where ϕ_0 is the desired phase shift. This can be achieved by defining a penalty function and then finding its minimum as a function of the parameters. As an example, we investigated $\phi(\omega)$ with parameters optimised for $\phi_0 = -\pi/2$ when the central frequencies are unmodified and only the Q-factor parameters are optimised. This was achieved by utilising the ROOT Minuit2 framework (version 6.28), where a penalty function χ^2 was defined as the squared relative deviation of $\phi(\omega)$ and ϕ_0, integrated over the relevant frequency range:

$$\chi^2 = \int_{\omega_{min}}^{\omega_{max}} \frac{(\Phi_A(\omega) - \Phi_0)^2}{{\Phi_0}^2} d\omega$$

The minimal deviation (i.e., the optimal χ^2) in the range defined via $\omega_{min} = 1$ Hz and $\omega_{max} = 100$ kHz was achieved with the following set of values:

$$Q_{1,A} = 0.913,\ Q_{2,A} = 0.721,\ Q_{3,A} = 0.819$$

$$Q_{1,B} = 0.807,\ Q_{2,B} = 0.683,\ Q_{3.B} = 0.802$$

As expected, a flatter, but still substantially oscillating $\phi(\omega)$ was achieved compared to the previous unoptimized case, as shown in Figure 8 (focused on the important frequency range from 15 Hz to 16,000 Hz).

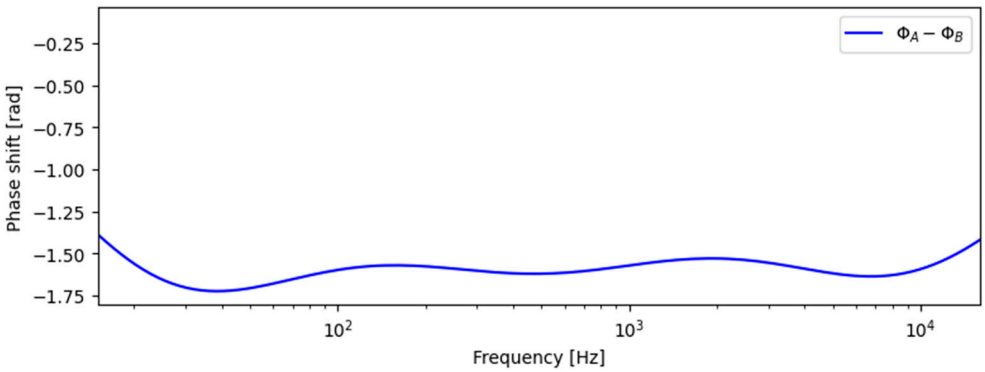

Figure 8. Phase difference as a function of frequency with parameters optimised for $\phi_0 = -\pi/2$.

In contrast to this, e.g., for $\phi_0 = -0.259$, an even flatter $\phi(\omega)$ can be achieved (see Figure 9) with

$$Q_{1,A} = 0.0449,\ Q_{2,A} = 0.172,\ Q_{3,A} = 0.169,$$

$$Q_{1,B} = 0.0638,\ Q_{2,B} = 0.189,\ Q_{3.B} = 0.131.$$

One may note, however, that the parameters listed above have huge uncertainties. The uncertainty here means that the given parameter can be varied within an interval corresponding to the uncertainty, and the resulting χ^2 value, defined in terms of the variance of the relative deviation from the desired constant phase shift, will change only by up to one unit. Hence, an equally constant phase shift can be achieved with significantly different parameters, but these need to be co-varied. Thus, it is clear that the parameters can be varied in broad intervals to obtain a similar level of constantness of the phase shift. In other words, one can fix some of the parameters to almost arbitrary values, and then fit just the remaining ones. At the same time, a filter with fewer than three stages might be possible if its parameters are optimised. This suggests that instead of numerical optimization, an analytical calculation might also be feasible.

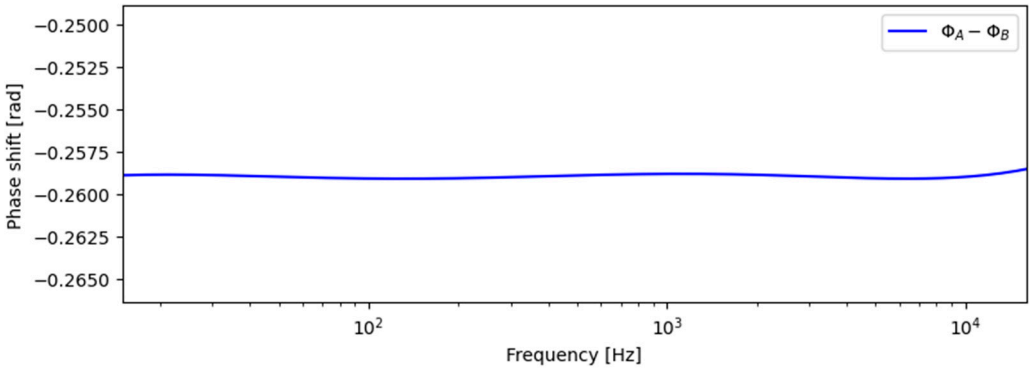

Figure 9. Phase difference as a function of frequency: the same as Figure 8, but optimised for $\phi_0 = -0.259$.

3.2. Analytic Calculations for the Single Stage Filter

To analytically investigate the form utilised in the previous section, we set two single-stage filters with the following frequency-dependent phase-shifts:

$$\phi(\omega) = -4 \cdot atan\left[(\omega/\omega_{0,A})^{-Q}\right] - 4 \cdot atan\left[(\omega/\omega_{0,B})^{-Q}\right] \tag{7}$$

where the central frequencies are different, but the Q exponents are identical. Utilising a series expansion technique, we found a good approximation of the above function in the following form:

$$\phi(\omega) \approx \phi_A(\delta) = \phi_{min} + D \cdot \delta^2 \tag{8}$$

with

$$\delta = ln(\frac{\omega}{\sqrt{\omega_{0,A}\omega_{0,B}}}),$$

$$\phi_{min} = 4 \cdot atan\frac{1}{2}\left\{(\frac{\omega_{0,B}}{\omega_{0,A}})^{\frac{-Q}{2}} - (\frac{\omega_{0,A}}{\omega_{0,B}})^{\frac{-Q}{2}}\right\},$$

and

$$D = \frac{4(\omega_{0,A}\omega_{0,B})^{Q/2}(\omega_{0,B}{}^{Q} - \omega_{0,A}{}^{Q})Q^2}{\omega_{0,A}{}^{2Q} + \omega_{0,B}{}^{2Q} + 2\omega_{0,A}{}^{Q}\omega_{0,B}{}^{Q}}$$

This approximation reflects that the $\phi(\omega)$ function above has an exact minimum, $\phi_{\min}$ at $\omega = \omega_{\min} \equiv \sqrt{\omega_{0,A}\omega_{0,B}}$, while the second derivative is related to D, defined above. This can be used to estimate the level of constantness of $\phi(\omega)$ near the minimum: the smaller the value of D, the more constant $\phi(\omega)$ is within a given vicinity of $\omega_{\min}$.

3.3. Analytical Optimization for the Single-Stage Filter

To optimise $\phi(\omega)$ in such a way that χ^2, quantifying the difference of $\phi(\omega)$ and ϕ_0, is minimised, we can define χ^2 by the following integral:

$$\int_{\omega_{min}}^{\omega_{max}} \frac{(\Phi(\omega) - \Phi_0)^2}{\Phi_0{}^2} d\omega \tag{9}$$

However, given the approximative shape (see Figure 8), this leads to a complex result. We instead define χ^2 via an integral on δ, defined in Equation (8), instead of ω:

$$\chi^2 = \int_{\delta_{min}}^{\delta_{max}} \frac{(\Phi_A(\delta) - \Phi_0)^2}{\Phi_0{}^2} d\delta \tag{10}$$

where

$$\delta_{min/max} = ln(\frac{\omega_{min/max}}{\sqrt{\omega_{0,A}\omega_{0,B}}}).$$

We find that χ^2 can be readily expressed in terms of the integration range $\omega_{\min}$ and $\omega_{\max}$ and the original parameters Q, $\omega_{0,\,A}$, and $\omega_{0,\,B}$ ('hidden' in D and $\phi_{\min}$), as:

$$\chi^2 = \frac{3D^2({\delta_{max}}^5 - {\delta_{min}}^5) - 10D({\delta_{max}}^3 - {\delta_{min}}^3)(\Phi_0 - \Phi_{min}) - 15(\delta_{max} - \delta_{min})(\Phi_0 - \Phi_{min})^2}{{\Phi_0}^2} \quad (11)$$

However, this expression is still complex, especially when D and $\phi_{\min}$ are substituted back into it.

In addition, one may observe that there is no unique minimum of this χ^2 even if one of the variables is fixed (see Figure 10).

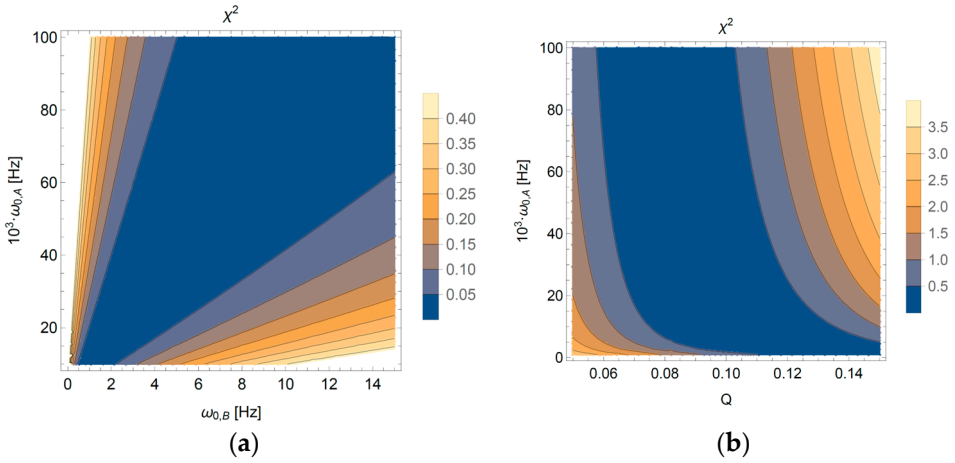

Figure 10. Plots showing χ^2 as (**a**) a function of $\omega_{0,A}$ and $\omega_{0,B}$ with $Q = 0.09$ and (**b**) a function of Q and $\omega_{0,B}$ with $\omega_{0,A}$= 3.5 Hz. The deep blue 'valleys' on both plots represent the set of minima.

These plots illustrate that there is no single strong minimum on the χ^2 map; instead, a valley of minima is present, and no single best set of parameters can be found. This also implies that some combinations of the parameters represent weak modes of the χ^2, while other combinations represent strong modes, i.e., significant parameter combinations. Further exploration into these parameter combinations is thus required.

3.4. Approximative Method for the Analytical Solution of the Single-Stage Filter

Instead of numerically minimising the above-defined χ^2, we explore analytical possibilities as well. Equation (8) introduces an approximate formula for $\phi(\omega)$, expressed via auxiliary variables δ, $\phi_{\min}$, and D, which allows us to, both directly and analytically, explore the deviation of $\phi(\omega)$ from a given ϕ_0. On the other hand, its average can be assessed easily if the desired interval is logarithmically centred around $\delta = 0$, i.e., $\omega_{\min}$ $\omega_{\max}$= $\omega_{0,A}$ $\omega_{0,B}$, and hence, $\delta_{\min} = -\delta_{\max} = ln\sqrt{\omega_{min}/\omega_{max}}$. In this case, the average of $\phi(\delta)$ (defined as $\langle\phi\rangle$) can be set to be equal to the desired ϕ_0, and this relation can be expressed as:

$$\phi_0 = \langle\phi\rangle = \phi_{min} + \frac{D}{3}({\delta_{min}}^2 + \delta_{min}\delta_{max} + {\delta_{max}}^2) = \phi_{min} + \frac{D}{3} \cdot \left(ln\sqrt{\omega_{min}/\omega_{max}}\right)^2 \quad (12)$$

Furthermore, the deviation from this average is determined by D, since the function is quadratic in δ, and its second derivative in δ is $2D$. We can quantify the non-flatness of $\phi(\omega)$ as the difference of $\phi_A(\delta)$ and $\phi_{\min}$ at $\delta_{\min}$ (or equivalently at $\delta_{\max}$). This difference can be analytically expressed with $\omega_{\min}$ and $\omega_{\max}$ as:

$$\Delta\phi = D \cdot \left(ln\sqrt{\omega_{max}/\omega_{min}}\right)^2 \quad (13)$$

Note that, because ω_{min} and ω_{max} are constants, the minimum $\Delta\phi$ is achieved when D is also minimal, and due to the squared logarithm, $\omega_{min}/\omega_{max}$ is equivalent to its inverse in this formula.

Furthermore, the above-mentioned centring around $\delta = 0$ allows us to declare two auxiliary variables, ω_0 and ξ, and express $\omega_{0,\mathrm{A}}$ and $\omega_{0,\mathrm{B}}$ in terms of them:

$$\omega_0 = \sqrt{\omega_{min}\omega_{max}} = \sqrt{\omega_{0,A}\omega_{0,B}} \tag{14}$$

with

$$\omega_{0,A} = \frac{1}{\xi} \cdot \omega_0,$$

$$\omega_{0,B} = \xi \cdot \omega_0, \text{ i.e., } \xi = \sqrt{\frac{\omega_{0,B}}{\omega_{0,A}}}.$$

The quantities $\phi_{\min}$, D and δ can therefore be expressed as

$$\phi_{\min} = 4 \cdot atan\left[\frac{1}{2}\left\{\xi^{-Q} - \xi^{Q}\right\}\right] \tag{15}$$

$$D = 4Q^2 \frac{\xi^{Q} - \xi^{-Q}}{2 + \xi^{2Q} + \xi^{-2Q}} \tag{16}$$

$$\delta = ln\frac{\omega}{\omega_0} \tag{17}$$

Hence, the approximate formula becomes

$$\phi(\omega) \approx 4 \cdot atan\left[\frac{1}{2}\left\{\xi^{-Q} - \xi^{Q}\right\}\right] + 4Q^2 \frac{\xi^{Q} - \xi^{-Q}}{2 + \xi^{2Q} + \xi^{-2Q}} \cdot \left(ln\frac{\omega}{\omega_0}\right)^2 \tag{18}$$

and the level of constantness is controlled by $\Delta\phi$, as defined above, and can now be expressed as:

$$\Delta\phi = 4Q^2 \frac{\xi^{Q} - \xi^{-Q}}{2 + \xi^{2Q} + \xi^{-2Q}} \cdot \left(ln\sqrt{\frac{\omega_{max}}{\omega_{min}}}\right)^2 = Q^2 \frac{\xi^{Q} - \xi^{-Q}}{2 + \xi^{2Q} + \xi^{-2Q}} \cdot \left(ln\frac{\omega_{max}}{\omega_{min}}\right)^2. \tag{19}$$

From these equations, it is apparent that there is no single optimal solution. Instead, a sufficiently flat phase shift can be found along the constant values of D as a function of Q and ξ, as shown in Figure 11 for $Q \in [0.04, 0.10]$ and $\xi \in [1, 100]$.

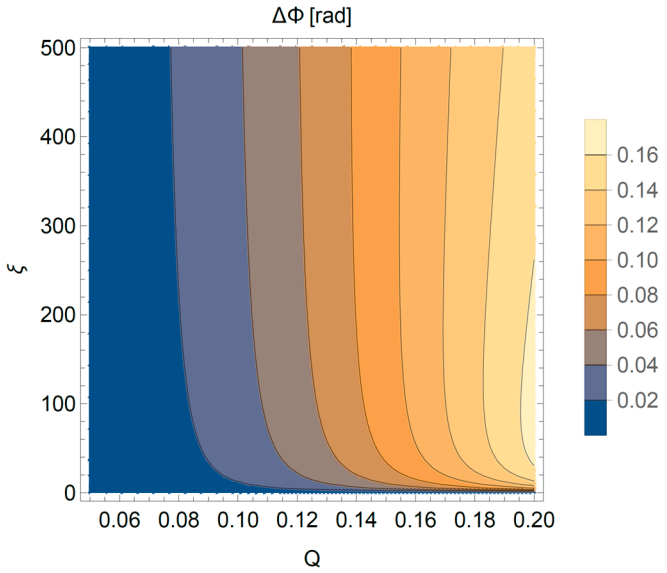

Figure 11. Plot showing $\Delta\phi$ as a function of Q and ξ. The deep blue region contains the most optimal solutions.

It can be seen from Figure 11 that the range of minimal $\Delta\phi$ is found when either Q or ξ is very small (note that here, Q goes from 0.04 to 0.10 and ξ goes from 1 to 100), and the actual minimum is at the edge of these boundaries and would be even smaller if Q or ξ were smaller.

However, we first need to determine the average phase shift as a function of Q and ξ, as the goal is not just a flat phase-shift (small $\Delta\phi$ in general), so $\phi(\omega)$ should also be centred around a given ϕ_0 value. This average is given in Equation (12) and can be expressed utilising the expressions of Equations (15) and (16), as follows:

$$\phi_0 = 4 \cdot atan\left[\frac{1}{2}\left\{\xi^{-Q} - \xi^{Q}\right\}\right] + \frac{1}{3}Q^2 \frac{\xi^{Q} - \xi^{-Q}}{2 + \xi^{2Q} + \xi^{-2Q}} \cdot \left(ln\frac{\omega_{max}}{\omega_{min}}\right)^2. \quad (20)$$

The above formula of Equation (20) is shown in Figure 12 for $\omega_{\max}/\omega_{\min} = 1200$ (true if the range is, e.g., 15 Hz to 18 kHz) as a function of Q and ξ, similarly to Figure 11.

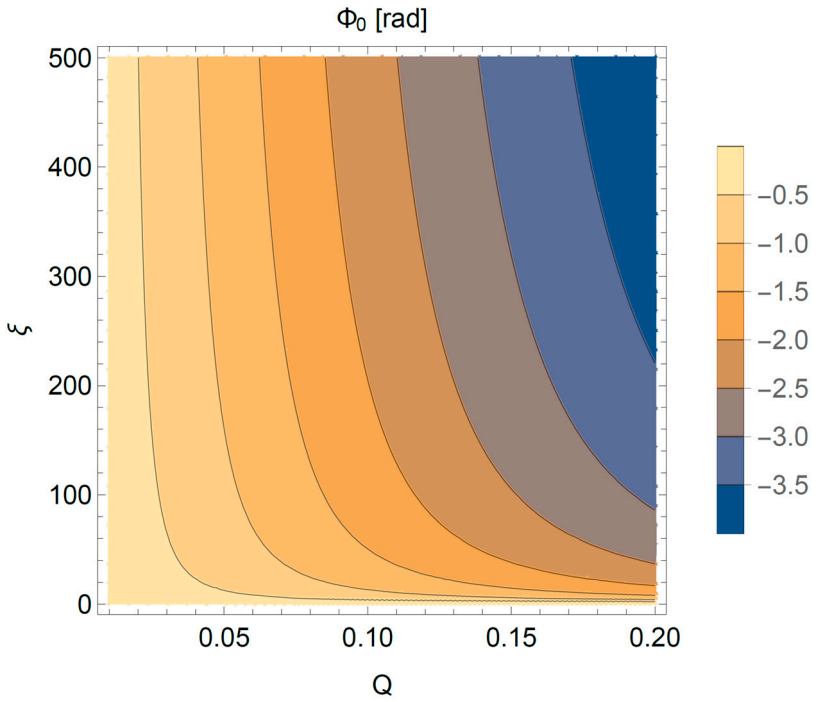

Figure 12. Plot showing ϕ_0 as a function of Q and ξ. Each of the lines corresponds to a given ϕ_0, i.e., ϕ_0 is constant along them.

To obtain a flat phase shift, a given line of constant ϕ_0 is chosen on Figure 12, representing a set of (ξ, Q) points. The minimal deviation is then found based on the $\Delta\phi$ map shown in Figure 11. However, as already mentioned above, the optimal $(\xi\ , Q)$ values are such that one of them is extremely small and, therefore, not practically feasible. Thus, instead of the smallest possible $\Delta\phi$, the smallest practically achievable $\Delta\phi$ is found.

These steps require us to solve Equation (20), for example, for ξ and then $\Delta\phi$, as expressed in Equation (19), resulting in the desired $(\xi\ , Q)$ point. This is very easy to do numerically, but less so analytically. Therefore, we explore numerical calculations.

3.5. Numerical Solution of the Approximative Case for the Single-Stage Filter

As mentioned above, to obtain the necessary (ξ, Q) points that result in $\langle\phi(\omega)\rangle = \phi_0$, we needed to solve Equation (20) in the case of a fixed ϕ_0, for an arbitrary Q value. Given $[\omega_{\min}, \omega_{\max}] = [15\ Hz,\ 20\ kHz]$ as the optimization range, ξ values providing this solution for $Q \in [0.1, 0.5]$ and $\phi_0 \in [5°, 90°]$ in the form of a $\xi(Q)$ function are shown in Figure 13 (and the values are given in Appendix A).

This gives us the required ξ value for any Q to have $\langle \phi(\omega) \rangle = \phi_0$. It is immediately apparent that, for small Q values, the required ξ becomes very large. Recall that ξ is used to calculate the central frequencies as $\omega_{0,A} = \omega_0/\xi$ and $\omega_{0,B} = \xi\omega_0$, where $\omega_0 = \sqrt{\omega_{min}\omega_{max}} \approx 548\ Hz$ in this case. Hence, ξ above a few hundred leads to $\omega_{0,B}$ in the MHz range, and these ξ values are not feasible in a digital implementation, which limits the possible Q range depending on ϕ_0. For example, in the case of $\phi_0 = -90°$, ξ becomes unfeasibly high at $Q = 0.1$ or below, while for $\phi_0 = -10°$, even $Q = 0.1$ yields usable ξ values. Regardless of this, with the required ξ values given for any Q, we can investigate the optimal Q.

Recall that the level of constantness is controlled by $\Delta\phi$, expressed in Equation (19), and this can now be evaluated as a function of Q only (with the $\xi(Q)$ value of the above plot for the given Q). Let us also recall that $\Delta\phi$ is the difference of $\phi(\omega)$ from $\phi_{\min}$ at $\omega_{\min}$ and at $\omega_{\max}$, so it is more meaningful in this case to plot $\Delta\phi/\phi_0$, as this represents the amplitude of the oscillations within the interval. Furthermore, recall that $\Delta\phi$ is the amplitude of $\phi(\omega)$, so the average deviation from ϕ_0 is lower than that.

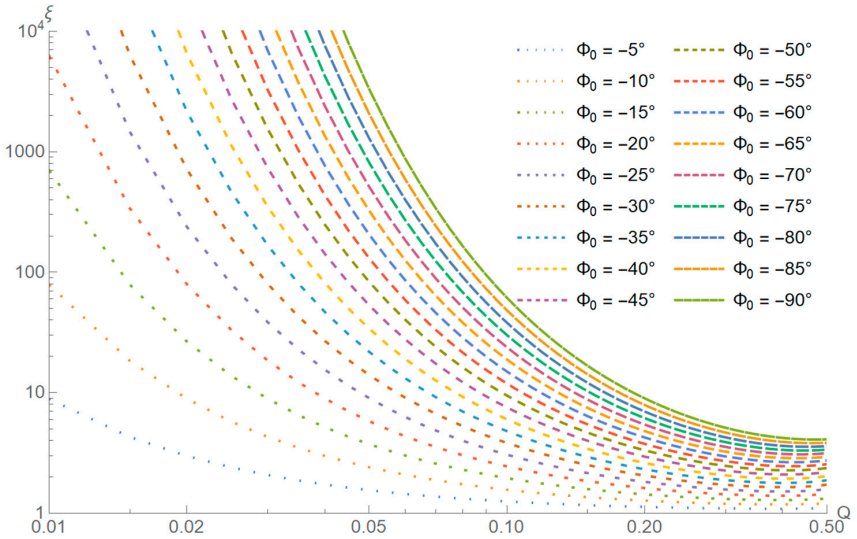

Figure 13. Lines in this plot represent $\xi(Q)$ functions solving Equation (20) in the case of a given ϕ_0, expressed in degrees for clarity.

In Figure 14, for $[\omega_{\max}, \omega_{\min}] = [15\ Hz,\ 20\ kHz]$, the relative amplitudes $\Delta\phi/\phi_0$ are shown as a function of Q (utilizing the $\xi(Q)$ shown in Figure 13) for various ϕ_0 values.

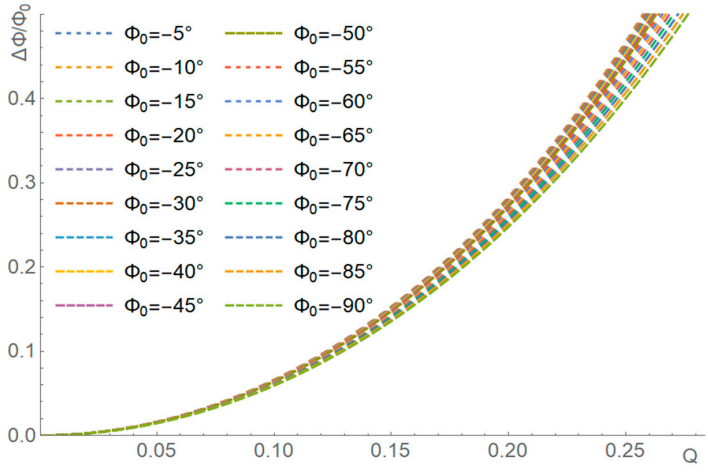

Figure 14. Relative amplitude $\Delta\phi/\phi_0$ as a function of Q for various ϕ_0 values.

There is an approximate quadratic increase in the $\Delta\phi/\phi_0$ of Q, which is evident if one plots the above data on a log–log plot. However, the important conclusion appears to be that there is no single optimal Q, but the smaller the value of Q, the more constant $\phi(\omega)$ becomes. If we aim to have a maximum deviation of 5%, then we can choose Q values up to 0.1, depending on ϕ_0. So, although we can choose the value of Q, it is important to note that the choice of Q determines the level of constantness. To obtain the desired $\langle\phi(\omega)\rangle = \phi_0$, the $\xi(Q)$ values need to be determined from Figure 13. We can therefore select a given Q value and then calculate the required $\xi(Q)$ values to obtain a mean equal to ϕ_0. This is shown for a few Q values in Figure 15.

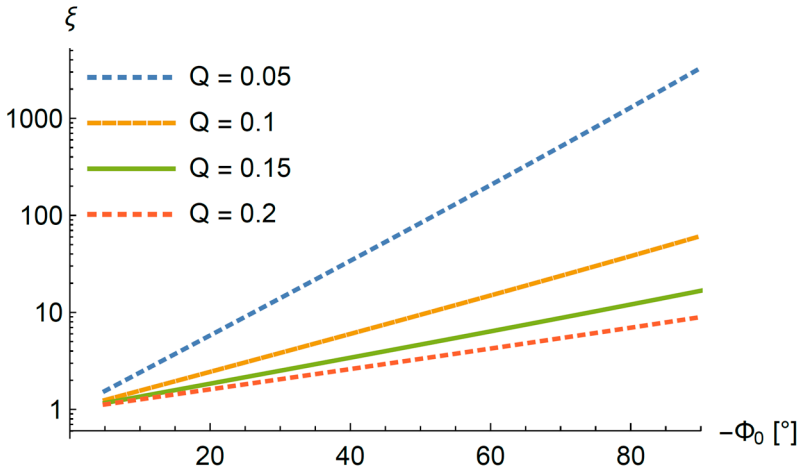

Figure 15. The ξ value required for $\langle\phi(\omega)\rangle = \phi_0$ as a function of ϕ_0 for four different Q values.

For example, in the case where $\phi_0 = -90°$, a choice of $Q = 0.1$ requires that we use $\xi \approx 61.3$ (the exact value is known from the above detailed calculation), and this will lead to an amplitude of $\Delta\phi/\phi_0 \approx 5\%$. To give more examples for $\phi_0 = -90°$, in the case of three concrete Q choices, one finds the following ξ values, corresponding to central frequencies based on Equations (15) and (16) (with $\omega_0 \approx 548\ Hz$, as mentioned above) and relative amplitudes:

$$Q = 0.05,\ \xi \approx 3312, \omega_{0,A} \approx 0.16\ Hz, \omega_{0,\mathrm{B}} \approx 1814\ kHz \text{ and } \Delta\phi/\phi_0 \approx 1.5\%$$

$$Q = 0.10,\ \xi \approx 61.3, \omega_{0,A} \approx 8.93\ Hz, \omega_{0,\mathrm{B}} \approx 33.58\ kHz \text{ and } \Delta\phi/\phi_0 \approx 5.9\%$$

$$Q = 0.15,\ \xi \approx 16.7, \omega_{0,A} \approx 32.8\ Hz, \omega_{0,\mathrm{B}} \approx 9.158\ kHz \text{ and } \Delta\phi/\phi_0 \approx 13.0\%$$

These are illustrated in Figure 16, confirming our calculations. In particular, it is important to note how the amplitude decreases with decreasing Q. This procedure can be repeated with any Q value, and the above calculations show the obtained $\omega_{0,\mathrm{A}}$ and $\omega_{0,\mathrm{B}}$ parameters and the resulting $\phi(\omega)$ amplitude $\Delta\phi/\phi_0$.

It is important to keep in mind that the smaller the value of Q is, the larger ξ has to be, but also the smaller $\Delta\phi/\phi_0$ becomes. Furthermore, the definition of $\Delta\phi/\phi_0$ corresponds to the deviation of $\phi(\omega)$ from its minimal value (reached when $\omega = \sqrt{\omega_{min}\omega_{max}}$) at the edges of the $[\omega_{\mathrm{min}}, \omega_{\mathrm{max}}]$ interval. The maximal deviation from ϕ_0 is actually smaller than that.

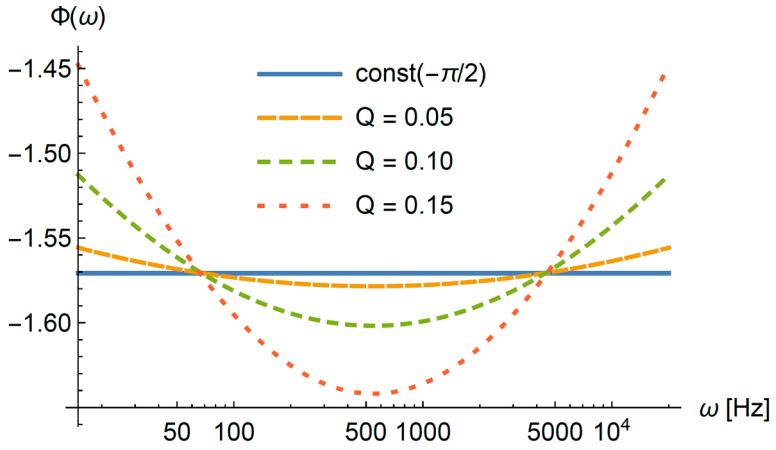

Figure 16. Phase difference as a function of frequency for three different Q values.

3.6. Numerical Solution for the Three-Stage Filter

As detailed above, the single-stage filter case around $\phi_0 = -90°$ requires very small Q values and very large ξ values and central frequencies. This motivates us to utilise more stages. It turns out that a two-stage filter yields equivalent results to the single-stage filter: the numerically optimal two-stage filter is obtained when the two central frequencies coincide. If these central frequencies do not coincide, then one needs a third filter to 'flatten out' the phase shift. Motivated by this, we try to solve the three-stage filter case, where:

$$\phi(\omega) = \phi_1(\omega) + \phi_2(\omega) + \phi_3(\omega) \tag{21}$$

Utilising the approximative formula of Equation (20) for each of the filters as follows

$$\phi_i(\omega) \approx 4 \cdot atan\left[\frac{1}{2}\left\{{\xi_i}^{-Q_i} - {\xi_i}^{Q_i}\right\}\right] + 4Q_i^2 \frac{{\xi_i}^{Q_i} - {\xi_i}^{-Q_i}}{2 + {\xi_i}^{2Q_i} + {\xi_i}^{-2Q_i}} \cdot \left(ln\frac{\omega}{\omega_{0i}}\right)^2 \tag{22}$$

leaves us with the following nine parameters: $Q_1, Q_2, Q_3, \xi_1, \xi_2, \xi_3$ and $\omega_{0,1}, \omega_{0,2}, \omega_{0,3}$. The central frequencies $\omega_{0,\mathrm{A,i}}$ and $\omega_{0,\mathrm{B,i}}$ can be calculated similarly to Equations (15) and (16).

Further investigation of the amplitude of $\phi(\omega)$ defined in Equation (21) reveals that many of the parameters are highly correlated. To achieve a symmetric $\phi(\omega)$ in the desired frequency range, it can be empirically found that the optimal choice (in terms of the simplicity of the formulas and symmetry of $\phi(\omega)$) is to set the following constraints as follows:

$$Q_3 = Q_1,\ \xi_3 = \xi_1,\ \omega_{0,2} = \omega_{0,1}\frac{\xi_2}{\xi_1},\ \omega_{0,3} = \omega_{0,1}{\xi_2}^2.$$

This leaves us with five free parameters: $Q_1, Q_2,\ \xi_1,\ \xi_2, \omega_{0,1}$, which are still correlated. Further empirical investigation of the level of constantness of $\phi(\omega)$ finds that three of these $(Q_1, \xi_2, \omega_{0,1})$ can be fixed to almost arbitrary values (i.e., these represent weak modes), as long as the remaining two (Q_2, ξ_1, representing strong modes) are set appropriately. These remaining two have to be set such that the desired $\phi(\omega) \approx \phi_0$ is reached. When the original formula of Equation (7) is utilised (not the above approximation of Equation (22)), the optimal choice of parameters is as follows (with ϕ understood in radians):

$$Q_1 = P_1,\ Q_2 = P_2 \cdot \Phi_0,\ \omega_{0,1} = O_1,$$

$$\xi_1 = 1 + X_1 \cdot \phi_0 + X_2 \cdot \phi_0^2 - X_3 \cdot \phi_0^3,\ \xi_2 = X_4,$$

where:

$$P_1 = 0.873,\ P_2 = -0.06661,\ O_1 = 10.668\ Hz,$$

$$X_1 = 0.00063792,\ X_2 = 0.0023086,\ X_3 = 0.0066800,\ X_4 = 44.595$$

The original central frequencies can thus be calculated from these parameters based on Equations (15) and (16). Furthermore, we find that the best result can be achieved if a small residual correction is applied, i.e., for Q_2 and ξ_1, a slightly modified ϕ_0 value is substituted. This correction can be expressed (with ϕ_0 in radians) as:

$$\phi_0^{(corr)} = 0.0054919 \cdot \phi_0^3 - 0.0030961 \cdot \phi_0^2 + 0.98601 \cdot \phi_0 - 0.00044568 \quad (23)$$

With this choice, a relatively constant $\phi(\omega)$ can be achieved for several ϕ_0 values, as illustrated in Figure 17. The absolute deviation from the desired ϕ_0 value is also shown in Figure 17. Clearly, deviations increase as ϕ_0 increases, but they are always below 0.5°. Most probably, the parameter values and functions can be numerically optimised further if required by the application.

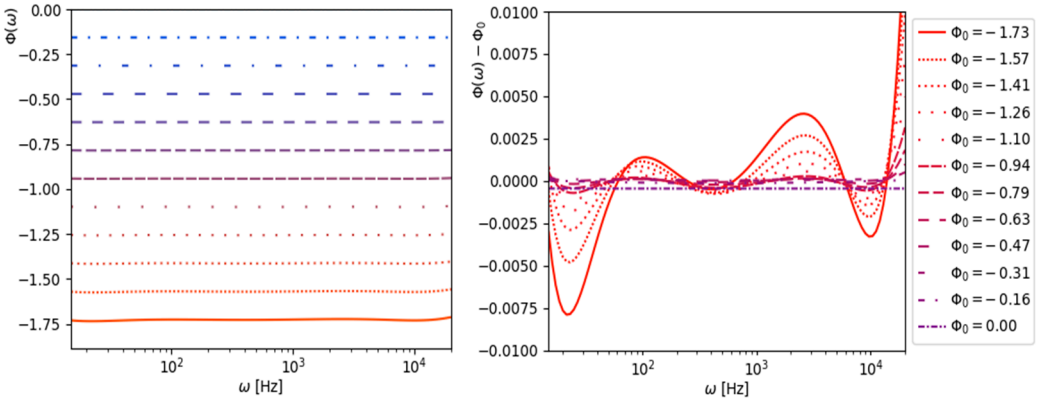

Figure 17. Left: Numerically optimised $\phi(\omega)$ curves for ϕ_0 values from $-9°$ to $-189°$ in $9°$ increments (shown in units of radian). Right: The absolute deviation (in degrees) from the desired ϕ_0 value.

Values for the parameters $Q_i, \xi_i, \omega_{0,i}$, as well as $\omega_{0,\mathrm{A,i}}$ and $\omega_{0,\mathrm{B,i}}$, for several ϕ_0 choices are given in Appendix B. One may note here that ξ_1 (and with that ξ_3) is extremely close to 1 for $|\phi_0| < 20°$. In fact, ξ_1 is even slightly lower than 1, but this is a numerical artefact. In fact, for these cases, it can be understood that $\xi_1 = \xi_3 = 1$. This also means that filters number 1 and 3 are effectively cancelled, and only filter number 2 remains in use. At this point, we can recall from the previous section that the single-stage filter was quite effective for smaller absolute values of ϕ_0. Here, it turns out that even with three filters, the above-described, partly intuitive numerical optimization does cancel two of them. They become important for $|\phi_0|$ values above approximately 20°, and especially near 90°.

4. Discussion

We now have the optimal parameters for a single-stage and a three-stage filter as well, so it is adequate to investigate their performances in terms of the constancy of the phase shift. A comparison of the single-stage and three-stage filters for $\phi_0 = -\pi/2$ is shown in Figure 18. Here, the single-stage filter parameters were calculated based on the previous section, with $Q = 0.1$ and $Q = 0.05$, and the interpolator was used to find the correct value for ξ (which is $\xi = 61.31$ in the former case, $\xi = 3312$ in the latter one) corresponding to $\omega_{0,B}$ of 33.6 kHz and 1.814 MHz, i.e., quite large values which are potentially unattainable in a digital implementation. On the other hand, for the three-stage filter, central frequencies are always <22 kHz. This underlines that, for $\phi_0 = -\pi/2$, the three-stage filter provides a much better solution than the single-stage one.

The codes implementing the above are given in [19] and can be readily used to implement the optimised three-stage filter.

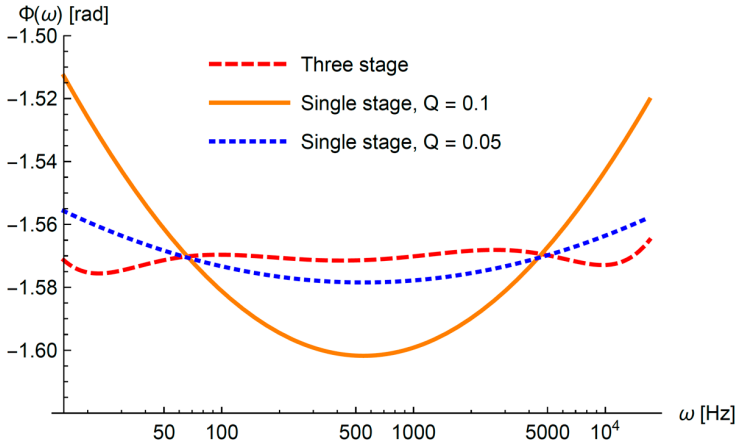

Figure 18. Comparison of the numerically optimised three-stage filter and two single-stage filters for Q = 0.1 and Q = 0.05.

5. Conclusions

In this paper, we present a new, frequency-independent phase shift technique that reduces the number of stages needed, and instead, we introduce the Q-factor as a variable which can be adjusted accordingly for the desired outcome. The accuracy of the technique presented here is dependent on both the frequency and the desired phase shift, with both higher and lower frequencies giving less accurate results. We find a relatively simple analytical formula for the single-stage filter, for which the optimal parameters are found numerically for the range of desired phase shifts [0–90°]. However, for the single-stage filter to be adequately uniform, unfeasibly large central frequencies have to be utilised for phase shifts above approximately 20°. In order to overcome this, a three-stage filter is introduced, and its optimal parameters are provided. In this case, the central frequencies for each of the filters are always below 22 kHz, providing a feasible possibility to implement a frequency-independent phase shift. We find that the three-stage filter is the best choice and that the numerical solution is adequate.

Author Contributions: Conceptualization, P.O.; Data curation, P.O., M.C. and A.K.F.V.B.; Formal analysis, A.K.F.V.B. and M.C.; Funding acquisition, P.O.; Investigation, P.O., A.K.F.V.B. and M.C.; Methodology, A.K.F.V.B. and M.C.; Project administration, P.O.; Resources, P.O.; Software, M.C.; Supervision, P.O.; Validation, M.C.; Visualization, M.C.; Writing—original draft, A.K.F.V.B. and M.C.; Writing—review and editing, A.K.F.V.B., M.C. and P.O. All authors have read and agreed to the published version of the manuscript.

Funding: This research received no external funding.

Data Availability Statement: The original contributions presented in the study are included in the article, further inquiries can be directed to the corresponding author/s.

Conflicts of Interest: A.K.F.V.B is from The Works Research Institute B. V. (company), other authors declare no conflicts of interest.

Appendix A

Table A1. The following table, corresponding to the $\Phi_0 = -\pi/2$ case, lists the ξ values for various Q values obtained from Equation (15) and plotted on Figure 11. Values for other Φ_0 mean phase shifts with a finer binning in Q are available as a text file in [19].

Q	ξ	Q	ξ	Q	ξ	Q	ξ	Q	ξ	Q	ξ
0.01	3.27·1017	0.11	42.868	0.21	8.2220	0.31	4.9613	0.41	4.1762	0.01	3.27·1017
0.02	5.79·108	0.12	31.865	0.22	7.6131	0.32	4.8259	0.42	4.1470	0.02	5.79·108
0.03	7.04·105	0.13	24.828	0.23	7.1045	0.33	4.7072	0.43	4.1238	0.03	7.04·105

Table A1. *Cont.*

Q	ξ	Q	ξ	Q	ξ	Q	ξ	Q	ξ	Q	ξ
0.04	24,664	0.14	20.075	0.24	6.6755	0.34	4.6033	0.44	4.1062	0.04	24,664
0.05	3312.5	0.15	16.720	0.25	6.3107	0.35	4.5126	0.45	4.0938	0.05	3312.5
0.06	871.16	0.16	14.267	0.26	5.9982	0.36	4.4334	0.46	4.0861	0.06	871.16
0.07	336.39	0.17	12.418	0.27	5.7289	0.37	4.3647	0.47	4.0828	0.07	336.39
0.08	165.13	0.18	10.990	0.28	5.4957	0.38	4.3055	0.48	4.0836	0.08	165.13
0.09	95.137	0.19	9.8635	0.29	5.2929	0.39	4.2548	0.49	4.0881	0.09	95.137
0.1	61.311	0.2	8.9592	0.3	5.1160	0.4	4.2119	0.5	4.0960	0.1	61.311

Appendix B

Table A2. The following table lists the numerically optimized parameters of the three-stage filter for various Φ_0 values. These parameters are also available as a text file in [19], along with values for central frequencies $\omega_{0,A,i}$ and $\omega_{0,A,i}$ for $i = 1, 2, 3$, calculable from $\omega_{0,i}$ and ξ_i based on Equation (13).

Φ_0	Φ_0 [rad]	$\Phi_0^{(corr)}$	Q_1	Q_2	Q_3	ξ_1	ξ_2	ξ_3	$\omega_{0,1}$ [Hz]	$\omega_{0,2}$ [Hz]	$\omega_{0,3}$ [Hz]
−5°	−0.08727	−0.08652	0.87347	0.00576	0.87347	1.0000	44.5951	1.0000	10.668	475.75	21,215
−10°	−0.17453	−0.17266	0.87347	0.01150	0.87347	1.0000	44.5951	1.0000	10.668	475.74	21,215
−15°	−0.26180	−0.25889	0.87347	0.01724	0.87347	1.0001	44.5951	1.0001	10.668	475.68	21,215
−20°	−0.34907	−0.34524	0.87347	0.02300	0.87347	1.0003	44.5951	1.0003	10.668	475.57	21,215
−25°	−0.43633	−0.43172	0.87347	0.02876	0.87347	1.0007	44.5951	1.0007	10.668	475.40	21,215
−30°	−0.52360	−0.51836	0.87347	0.03453	0.87347	1.0012	44.5951	1.0013	10.668	475.14	21,215
−35°	−0.61087	−0.60518	0.87347	0.04031	0.87347	1.0019	44.5951	1.0020	10.668	474.79	21,215
−40°	−0.69813	−0.69219	0.87347	0.04610	0.87347	1.0029	44.5951	1.0030	10.668	474.34	21,215
−45°	−0.78540	−0.77943	0.87347	0.05192	0.87347	1.0041	44.5951	1.0042	10.668	473.77	21,215
−50°	−0.87267	−0.86691	0.87347	0.05774	0.87347	1.0055	44.5951	1.0056	10.668	473.07	21,215
−55°	−0.95993	−0.95466	0.87347	0.06359	0.87347	1.0073	44.5951	1.0074	10.668	472.23	21,215
−60°	−1.04720	−1.04270	0.87347	0.06945	0.87347	1.0094	44.5951	1.0095	10.668	471.24	21,215
−65°	−1.13446	−1.13104	0.87347	0.07534	0.87347	1.0119	44.5951	1.0120	10.668	470.09	21,215
−70°	−1.22173	−1.21972	0.87347	0.08124	0.87347	1.0148	44.5951	1.0148	10.668	468.78	21,215
−75°	−1.30900	−1.30876	0.87347	0.08717	0.87347	1.0181	44.5951	1.0181	10.668	467.28	21,215
−80°	−1.39626	−1.39816	0.87347	0.09313	0.87347	1.0219	44.5951	1.0218	10.668	465.59	21,215
−85°	−1.48353	−1.48797	0.87347	0.09911	0.87347	1.0262	44.5951	1.0259	10.668	463.71	21,215
−90°	−1.57080	−1.57820	0.87347	0.10512	0.87347	1.0310	44.5951	1.0306	10.668	461.62	21,215
−95°	−1.65806	−1.66885	0.87347	0.11116	0.87347	1.0364	44.5951	1.0357	10.668	459.32	21,215

References

1. Madihian, M.; Watanabe, K.; Yamamoto, T. A Frequency-Independent Phase Shifter. *J. Phys. E Sci. Instrum.* **1979**, *12*, 1031–1032. [CrossRef]
2. Jones, B.K.; Sharma, B.K.; Bidle, D.H. A Frequency-Independent Phase Shifter. *J. Phys. E Sci. Instrum.* **1980**, *13*, 1346–1347. [CrossRef]
3. Helfric, A. Phase Shifter Using Digital Techniques. *Electr. Des. News* **1987**, *32*, 289–290.
4. Mittal, M.; Jamuar, S.S. Programmable Frequency-Independent Switched-Capacitor Phase Shifter of Unity Gain. *Meas. Sci. Technol.* **1991**, *2*, 475–477. [CrossRef]
5. Cowan, B. A Versatile Phase Shifter for NMR Experiments and Other Applications. *Meas. Sci. Technol.* **1992**, *3*, 296–298. [CrossRef]

6. Jung, D.H.; Ha, I.J. Low-Cost Sensorless Control of Brushless DC Motors Using a Frequency-Independent Phase Shifter. *IEEE Trans. Power Electron.* **2000**, *15*, 744–752. [CrossRef]
7. Lobb, W.E. Acoustic Sound System for a Room. U.S. Patent 4,837,829, 6 June 1989.
8. Zurcher, F. Sound Acquisition Method and System, and Sound Acquisition and Reproduction Apparatus. U.S. Patent 5,524,059, 4 June 1996.
9. Elko, G.W.; Teutsch, H. Second-Order Adaptive Differential Microphone Array. *J. Acoust. Soc. Am.* **2004**, *115*, 14. [CrossRef]
10. Oomen, P.; De Klerk, L. Environmental Sound Loudspeaker. Netherlands, Amsterdam: Patent WO/2023/287291, 19 January 2023.
11. Sedra, A.S.; Smith, K.C. *Microelectronic Circuits*, 3rd ed.; Saunders College Publishing: Philadelphia, PA, USA, 1992.
12. Cherepov, S.V. Bridge for AC Measurement of Magnetic Susceptibility. *Instrum. Exp. Tech.* **1986**, *25*, 1226–1227.
13. Batrachenko, V.S.; Zarubina, T.V. Controllable Digital Phase Shifter. *Instrum. Exp. Tech.* **1978**, *21*, 1344–1345.
14. Maslov, N.V.; Prikhnenko, R.E. Digital Phase Shifter for a Precision Calibrator of Phase Shifts. *Instrum. Exp. Tech.* **1978**, *21*, 1346–1347.
15. Sankaran, P.; Jagadeesh Kumar, V.; Sudhakar Rao, K. Precision Frequency-Independent Variable-Phase Phase Shifter. *Electron. Lett.* **1995**, *31*, 154–155. [CrossRef]
16. Abuelma'atti, M.T.; Baroudi, U. A Programmable Phase Shifter for Sinusoidal Signals. *Act. Passiv. Electron. Compon.* **1998**, *21*, 107–112. [CrossRef]
17. Al-Absi, M.A. A Simple Low Cost Frequency-Independent Phase Shifter. *Arab. J. Sci. Eng.* **2009**, *34*, 145–152.
18. Bitar, M.A.; Gallo, A.; Volpe, F.A. Multi-Pole Multi-Zero Frequency-Independent Phase-Shifter. *Rev. Sci. Instrum.* **2012**, *83*, 114703. [CrossRef]
19. Csanád, M. Frequency Independent Phase Shifter. *GitHub*. 2023. Available online: https://github.com/theworksinstitute/fips (accessed on 25 May 2024).